Resistance of Coatings for Boiler Components of Waste-to-Energy Plants to Salt Melts Containing Copper Compounds

Mathias Christian Galetz, Johannes Thomas Bauer, Michael Schütze, Manabu Noguchi, and Hiromitsu Cho

(Submitted October 15, 2012; in revised form January 23, 2013)

The accelerating effect of heavy metal compounds on the corrosive attack of boiler components like superheaters poses a severe problem in modern waste-to-energy plants (WTPs). Coatings are a possible solution to protect cheap, low alloyed steel substrates from heavy metal chloride and sulfate salts, which have a relatively low melting point. These salts dissolve many alloys, and therefore often are the limiting factor as far as the lifetime of superheater tubes is concerned. In this work the corrosion performance under artificial salt deposits of different coatings, manufactured by overlay welding, thermal spraying of self-fluxing as well as conventional systems was investigated. The results of our studies clearly demonstrate the importance of alloying elements such as molybdenum or silicon. Additionally, the coatings have to be dense and of a certain thickness in order to resist the corrosive attack under these severe conditions.

1. Introduction

In waste incinerators one of the major reasons for corrosion is the deposition of hot ashes and salts, which can lead to severe attack even at relatively low temperatures. The feedstock in these plants determines the ash and salt composition and generally two qualities of waste have to be distinguished, the as-received "municipal solid waste" (MSW), which can be fed directly as collected into the plant or the "refuse-derived fuel" (RDF) waste, which is shredded and sorted in order to remove and recover valuable metal contaminants and also to concentrate combustible constituents such as plastics, organic matter, or pulp (Ref 1). The latter fuel has a higher heating value and improved operability characteristics and can be burned in a fluid bed boiler or grate-fired furnace. The efficiency and therefore energy harvest of this operation mode are higher, but the higher temperature and recirculation induce a high transfer of heavy metals into the fly ashes such as copper, zinc, antimony, tin, and lead, which accelerates corrosion (Ref 2).

Mathias Christian Galetz, Johannes Thomas Bauer, and **Michael Schütze**, Dechema Forschungsinstitut, Frankfurt Germany; **Manabu Noguchi**, Ebara Corporation Fluid Machinery & Systems Company, Chiba, Japan; and **Hiromitsu Cho**, Ebara Environmental Plant Co., Ltd., Tokyo, Japan. Contact e-mail: galetz@dechema.de.

Especially the copper content can vary significantly in the feedstock, with copper concentrations in RDF ranging up to 3200 mg/kg, compared to 2000 mg/kg in MSW (Ref 3, 4). During combustion of chlorine-rich waste, the amount of heavy metals transferred out of the fuel bed is especially high and can be directly related to the chlorine content in the fuel (Ref 1). In this case copper and other heavy metals are transported as chlorides with the flue gas, while in environments with low chlorine concentrations, typically 90-95% of the input copper is concentrated in the bottom ash (Ref 5). To make matters worse, approximately one half of the Cl-content of MSW is due to natural organic compounds, while the other half is due to chlorinated plastics (Ref 6), mostly polyvinylchloride (PVC). PVC often occurs in combination with copper, for example, in insulations of cables or rods. It was observed, that the presence of copper in the ashes and deposits can strongly accelerate the corrosion rate of critical components like superheater tubes (Ref 7).

Generally, salts and ashes from the flue gas sticks on the comparatively cold superheater tubes. On the outer scale of these deposits, the ashes usually contain mainly sulfates and oxides such as $CaSO_4$, Na_2SO_4, or K_2SO_4, but also heavy metal compounds, such as $ZnSO_4$ and $PbSO_4$. In contrast, close to the metal surface, the ash deposits usually contain high amounts of chlorine and the metals are present as chlorides such as $CaCl_2$, KCl, $ZnCl_2$, and $PbCl_2$ or $CuCl_2$. The insufficient conversion of chlorides into sulfates and oxides close to the surface, where the SO_2 and SO_3 contents and oxygen partial pressure are relatively low, can be associated with severe corrosive attack (Ref 2).

Heavy metal chloride salt melts of Na, Pb, K, Fe, Zn, or Ca compounds, which are often found in such deposits as have even lower melting points then sulfates, which are in

Table 1 Investigated coatings

| Substrate | Cladding | Thermal-sprayed coatings | | | Supplier |
		HVOF	Flame spray	Self-fluxing	
2.4856		NiCrAlY			ATZ Entwicklungszentrum
2.4856		NiCr20 + Cr3C2			ATZ Entwicklungszentrum
1.5415	2.4856				Castolin Eutectic
1.4952	…		2.4856		JB Industriemontagen
1.4952	…		JB007		JB Industriemontagen
1.5415	JB007				JB Industriemontagen
…	…			B0	Daiichi High Frequency
…	…			B1	Daiichi High Frequency

the range from 156 °C (NaCl-FeCl$_3$) to 475 °C (CaCl$_2$-PbCl$_2$), depending on the specific composition. CuCl$_2$ in its pure form melts at 622 °C, but also forms various eutectica with other chlorides e.g., CuCl$_2$-K$_2$CuCl$_3$ with a eutectic temperature of 360 °C (Ref 8). When in contact with metal, chlorides act in many corrosive ways to destroy the materials employed for boilers or other components. Chlorine can react directly with metals to form low-melting or volatile products. In such cases chlorine induces an extremely severe corrosion mechanism called ''active oxidation'', which is described in detail elsewhere (Ref 9). Other possible reactions are the penetration and dissolution of oxide scales.

Therefore, for superheater tubes, especially in such heavy metal-rich atmospheres, high-alloyed systems are required, which can, at least to a certain extent, cope with such conditions (Ref 7). Tubes from such alloys are not economically feasible, however, and have a low thermal conductivity; instead metallic coating options are being considered, which offer a reasonable corrosion resistance, good thermal conductivity, process ability, and price. They can be applied by the following techniques (Ref 1):

– Composite tubing consist of two layers, with the inner layer made of a boiler steel and the outer protective layer made of a highly corrosion resistant material.
– Surface welding or cladding, e.g., with Alloy 625, the most commonly used alloy for this purpose in waste-to-energy plants (WTP).
– Thermal spraying of resistant coatings, e.g., by flame, high velocity oxygen flame (HVOF), or atmospheric plasma spraying.
– A two-step spray and fuse process by which a coating material with brazing properties is deposited by thermal spray techniques and subsequently fused by heating above its melting point.

The coating materials contain a reservoir of different protective elements, such as chromium, silicon, or molybdenum. Those elements form barrier layers during exposition, which lead to separation of the salt from metal. In salt melts, it is of particular importance that these scales react slowly and do not dissolve in the ashes (Ref 9).

The aim of this study was to evaluate the behavior of different coating systems for boiler components exposed to salt ashes with and without high copper contents in

atmospheres above 500 °C, which is a temperature relevant for modern efficient boilers that use high steam parameters to achieve high efficiency.

2. Experimental Procedure

The resistance of several coatings to salt deposits at 540 °C was examined as well as the influence of copper chloride content in the ash on the corrosion behavior. As substrate material for the application of the different coatings 1.5415 (16Mo3) steel, 1.4952 (X6CrNiNbN-25-20) or 2.4856 (NiCr22Mo9Nb) were used. Commercial NiCrAlY and Cr3C2 + 25 wt.% NiCr20 powders (Sulzer Metco) were applied by ATZ Entwicklungszentrum via HVOF. Table 1 gives an overview of the examined materials and coatings as well as the supplier of the coatings. Additionally, Alloy 625, which is often used in WTPs, and a newly developed alloy from JB Industriemontagen, described in Ref 10 were investigated as flame-sprayed and overlay welded material.

JB 007, which is, in contrast to the other coatings not a nickel but cobalt-based system, and contains about 30 wt.% chromium, was flame-sprayed and cladded by JB Industriemontagen (Germany); 2.4856 was also flame-sprayed by JB Industriemontagen (Germany); cladding of the same material was conducted by Castolin Eutectic (Switzerland). From tube material, samples were cut and divided into pieces having surface areas of about 200 mm^2. Additionally, two self-fluxing heat-treated Cr-Si-B-Mo-Ni-base alloys (B0 and B1) were provided as free-standing coatings in the form of 10 × 10 × 2.4 mm thick plates from Daiichi High Frequency Co, Ltd. (Japan). B1 contains more chromium than B0, however, the exact composition of the coatings is proprietary and must not be revealed.

Before exposure, the surfaces of the samples were cleaned using an isopropanol ultrasonic bath. To investigate the influence of copper on the corrosion behavior two different artificial ashes were used. The composition of these two ashes is given in Table 2. Both were diluted with inert alumina particles to allow better gas penetration.

Ash B is analogous to the chemical composition with a similar chlorine/sulfate ratio as found in an actual WTP, which is fired using refuse-derived fuel, contaminated with up to an average of 3000 mg/kg copper in the waste

Table 2 Chemical composition of the two salt mixtures

	Salt A		Salt B	
	wt.%	Example of blending, g	wt.%	Example of blending, g
Al_2O_3	70.00	404.76	70.00	476.19
NaCl	4.61	26.65	3.92	26.65
Na_2SO_4	6.63	38.35	5.64	38.35
KCl	2.48	14.35	2.11	14.35
K_2SO_4	3.57	20.65	3.04	20.65
$CaCl_2$	7.41	42.86	6.30	42.86
$PbCl_2$	2.65	15.31	2.25	15.31
$ZnCl_2$	2.65	15.31	2.25	15.31
$CuCl_2$	0	0	4.50	30.61
total	100.00	578.23	100.00	680.27

(Ebara, unpublished data). In the ash deposits from this plant, $CuCl_2$ was enriched up to 4.5 wt.% close to the surface of the metal tubes. This amount was chosen for the laboratory tests and therefore corresponds to the salt that is in contact with the base material. The composition of ash A is similar to that of ash B, with the only difference being that no copper chloride was added to directly study its influence (see Table 2).

All samples were placed in alumina crucibles and about two-thirds of the sample were in contact with the artificial ash, the remaining third was directly exposed to a flowing gas with the composition $N_2 + 7\%$ $O_2 + 19\%$ $H_2O + 9\%$ $CO_2 + 5$ ppm $SO_2 + 800$ ppm HCl. The investigation was focused on such parts of the sample, which were fully immersed in the melt.

The testing temperature was 540 °C, which lies above the eutectic temperature for a mixture of KCl-NaCl-K_2SO_4-Na_2SO_4 (518 °C) completely free of any heavy metal compounds (Ref 11). As both salts contain additional Zn and Pb, which further lowers the melting point, it is ensured that the ashes are in the molten state at the temperature of exposure and the samples are well immersed in the salt melt. Samples were tested for 300, 700, and 1000 h. After each testing interval, the ash on the remaining samples was removed and a new batch of ash was applied to the samples. An ash composition typical for ashes in contact with the super heater tube surface was chosen for these tests. Such ashes are not in thermodynamic equilibrium with the flow gas and therefore slowly decompose into products with a composition that resembles the outer deposit on tubes, where the oxygen partial pressure is higher and metal sulfates and oxides are more stable than chlorides. During the test, the salt in the crucibles is also diluted with corrosion products and after each testing interval salt, which had been molten at temperature stuck to the sample surface. The corrosion rate was measured as an average of the initial coating thickness minus the residual coating thickness, determined from cross sections on different spots of the sample. Three measurements of the residual coating thickness were done in the area of the sample fully covered with salt. The coating thickness after the initial deposition was not constant over the sample length, neither for the thermal-sprayed coatings, nor for the overlay welded coatings. This inhomogeneity has to be kept in mind while interpreting the results.

Sub-coating migration of corrosive constituents during exposure is also a potential error, but can be excluded, as coating spallation was only observed in cases where the coating was already significantly corroded from the surface to the substrate interface.

The microstructure and morphology of the corrosion products were investigated using SEM and electron microprobe analysis (EMPA). The cross sections were prepared using a water-free preparation technique, as described in Ref 7 to avoid removal of chlorides. Porosity was determined from SEM pictures of the cross sections via image analysis (Image J), as described elsewhere (Ref 12). By this method, porosity is within a microstructure is detected due to the high degree of contrast between the dark pores (voids) and the more highly reflective coating material. It has been shown, that this method can reproducibly detect and measure microstructural features (pores, cracks, etc.) within thermal spray coatings (Ref 13).

3. Results and Discussion

In Fig. 1-6 selected coatings in their initial state and after 300 or 1000 h testing are shown. The thermally flame-sprayed and also the HVOF-sprayed coatings have either disappeared after 300 h (NiCr20 + Cr3C2, Fig. 1) or do not provide protection anymore (JB007, 2.4856) due to spallation shown exemplarily in Fig. 3 for sprayed 2.4856 or they expanded due to oxidation/corrosion to for a loose, porous layer (MCrAlY, Fig. 2). As chlorine penetrates the coating, a thick corrosion layer is formed between the substrate and coating. Therefore no examination of these coatings was done for longer exposure times than 300 h. The porosity of the coating in the initial state plays a crucial role as displayed in Fig. 7. The overlay welded coatings are not included in Fig. 7, because they did not reveal any porosity, see Fig. 5 and 6.

In the flame- and HVOF-thermally sprayed coatings the porosity occurs along splats, while in the coatings B0 and B1 it is a closed porosity with spherically shaped pores (Fig. 4). Corrosion advances especially along the pores
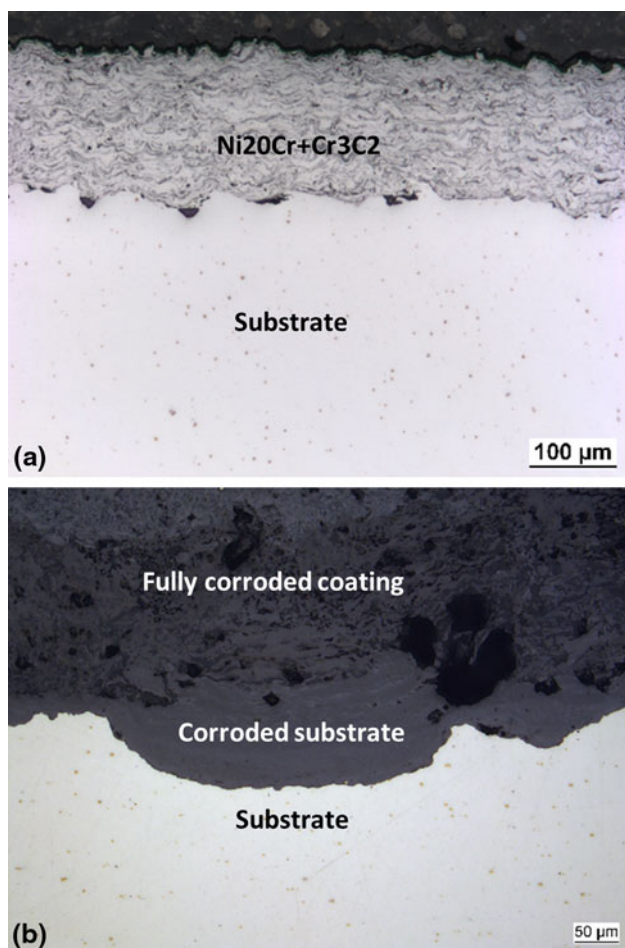
Fig. 1 NiCr20 + Cr3C2 (a) before exposure, (b) after 300 h in salt B

Fig. 2 NiCrAlY (a) before exposure, (b) after 300 h in salt A

between the splats in the thermally sprayed coatings, while both overlay welded coatings (B0 and B1) and the self-fluxing coating with the closed porosity are exclusively attacked from the surface (Fig. 1-6). These coatings neither showed any sign of internal corrosion nor any increased porosity or penetration.

In Fig. 8 the average corrosion rates after 1000 h are only reported. For those coatings, which were still dense and considered protective in both salt compositions after 300 h.

The corrosion rates in salt A were lower than in salt B in each case. This result demonstrates the strong influence of the copper chloride in the salt. The overlay welded coating 2.4856 showed the lowest susceptibility to the copper chloride, whereas the other coatings are strongly affected.

In salt B the thermally sprayed coatings were nearly completely consumed after 300 h, even the material 2.4856. In salt A where the attack was lower, the flame and HVOF thermal-sprayed coatings were porous and spalled off after 300 h. In conclusion, these coatings are not an option for the use in a plant, at least not as long as porosity and the splat-like structures are present in the coating.
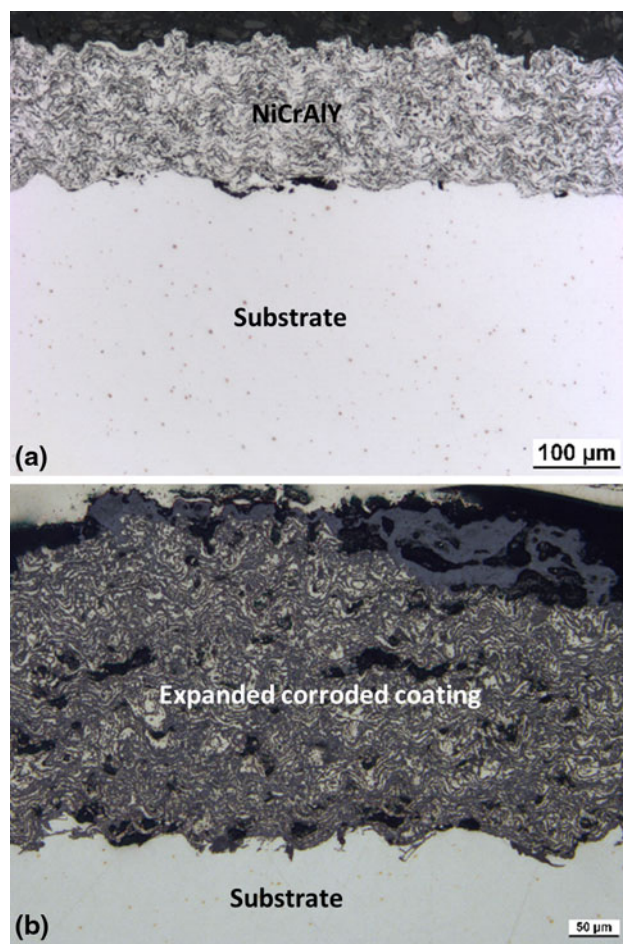
The critical porosity of the coatings could be lowered by an optimization of the coating process parameters, by a more advanced process or a pre-oxidation step in order to fill the pores with oxides since any porosity which is left offers a weak spot for the corrosive attack and penetration by chlorine.

– In salt A the thermally sprayed self-fluxing coating B0 shows the lowest corrosion rate of about 27.5 µm/100 h, whereas in salt B it is comparable to overlay welded alloy 625 (Fig. 8). Coating B1 in salt B was already disintegrated after 700 h. In the sprayed and fused coatings porosity was found as well (Fig. 7), but due to the self-fluxing properties of the alloys and the thermal treatment, the porosity was closed, which is much less detrimental (Fig. 5). Although the chemical composition also plays an important role, the homogeneous and slowly proceeding corrosion front proves that if a closed porosity is achieved, the properties of the thermally sprayed coatings potentially match those of overlay welded ones. In contrast to the other alloys, the sprayed and fused specimens B0 and B1 revealed an increased amount of porous and voluminous corrosion products in both salt mixtures. A thick layer consisting of a mixture
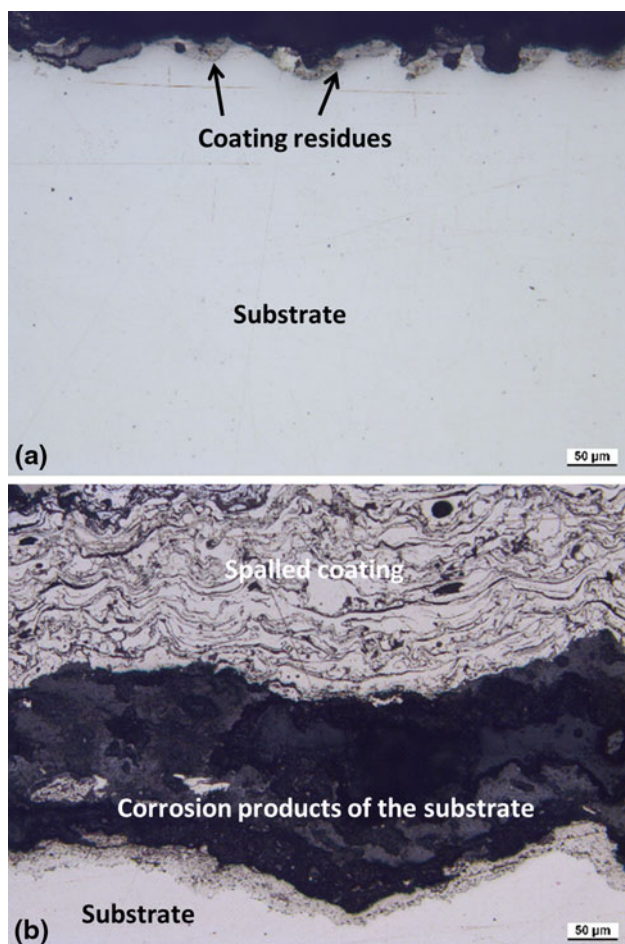
Fig. 3 Sprayed 2.4856 (a) after 300 h in salt B, (b) after 300 h in salt A

Fig. 4 Self-fluxing freestanding coating B0 (a) before exposure, (b) after 1000 h in salt B

of salt melt and oxides from the coating formed on the sample surface. The thickness could not be determined, however, as even careful handling of the specimen quickly lead to spallation due to the stickiness of the salt when the samples were removed from the crucibles. Therefore only the residual metal thickness is reported. To study the influence of certain alloying elements on the corrosive behavior of the coatings, electron microprobe analysis was conducted on the different samples: Welded 2.4856: Mo, S, and Cl were found at the corrosion front under a chromium rich scale as shown for salt B in Fig. 9.

– Welded JB007: Besides the aggressive elements Cu, Cl, and S from the salt, the elements Co and Si from the coating were enriched at the corrosion front in both salts, under a porous Fe- and Cr-rich oxide scale, as shown in Fig. 10.

– B0 and B1: Chlorine is present at the corrosion front and no continuous scale of elements of the substrate can be found at the corrosion front for both salts (Fig. 11). However, a non-continuous, yet obvious enrichment of the protective elements Cr and Si can be observed.
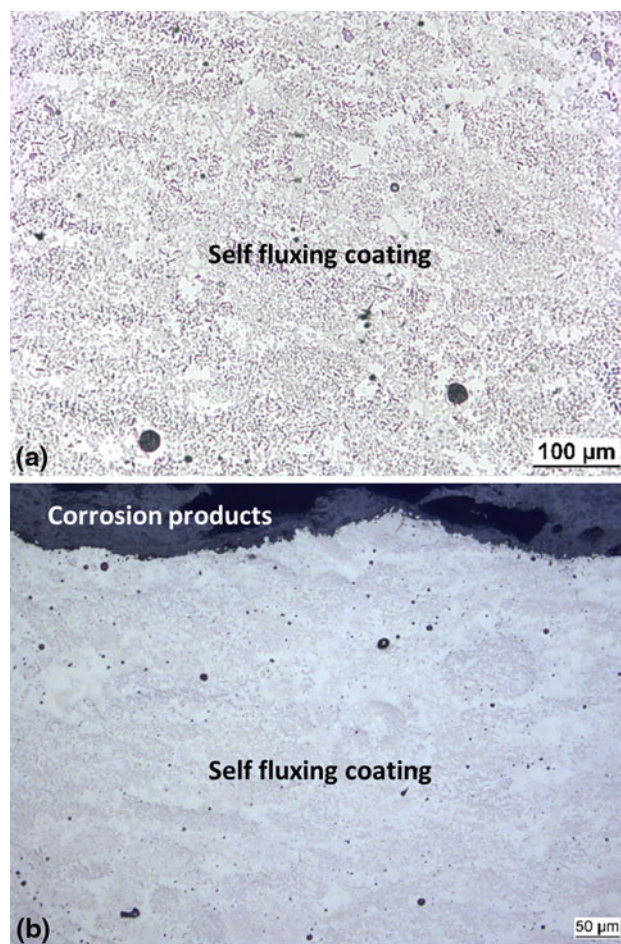
4. Discussion

Our studies on these coatings are consistent with the observation from actual plants, that it is hard to predict reliable corrosion rates even under constant operating conditions (Ref 6), because the actual corrosion rates highly depend on the composition of the feed and as a result, on the composition of the deposits, which can significantly accelerate the corrosion rate. In particular, the detrimental effect of the presence of copper chloride in the salt was proven in this study. In the salt-containing copper chloride, the corrosive attack is always more severe for all types of coatings than in the deposits that did not include any copper (Fig. 8). Several reasons have been suggested to explain the detrimental influence of heavy metals. A lowering of the melting points was observed and reported previously for the two salt mixtures used here, as the addition of $ZnCl_2$ and $PbCl_2$ to the KCl-$NaCl$-K_2SO_4-Na_2SO_4 eutectic mixture decreases the melting point by about 160 to 360 °C (salt A) and down to 290 °C if additional copper chloride is present (salt B) (Ref 7). A more fluid salt can penetrate oxides scales more easily and can infiltrate pores. Additionally, a catalyzing effect by the
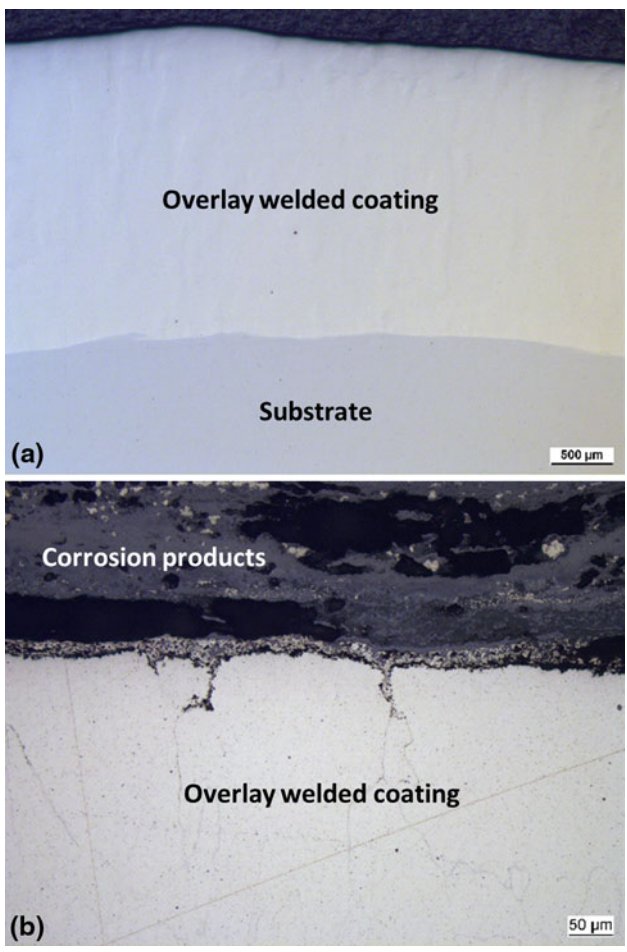
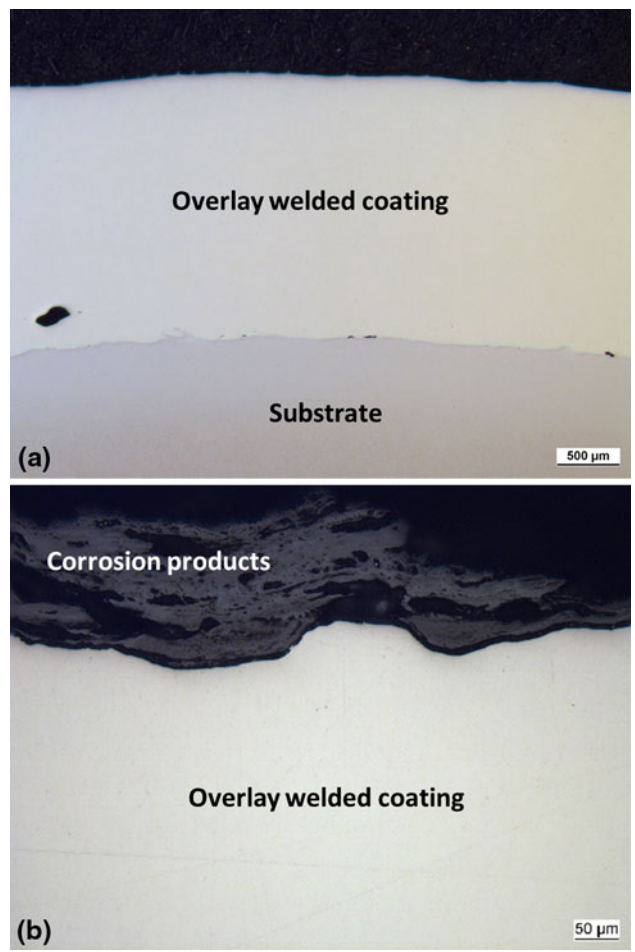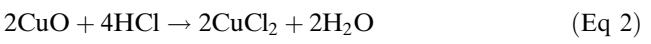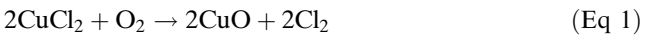**Fig. 5** Overlay welded JB007 (a) before exposure, (b) after 1000 h in salt B

Fig. 6 Overlay welded 2.4856 (a) before exposure, (b) after 1000 h in salt B

addition of copper (Ref 11, 14) can enhance the formation of elemental chlorine from HCl via the two-step Deacon reaction:

$$2CuCl_2 + O_2 \rightarrow 2CuO + 2Cl_2 \qquad (Eq\ 1)$$

$$2CuO + 4HCl \rightarrow 2CuCl_2 + 2H_2O \qquad (Eq\ 2)$$

A third detrimental influence was suggested to occur due to dissolution of chromia scales by the formation of chromate compounds with heavy metals. In accordance with the damage of Cr_2O_3 by lead (Ref 15, 16), a similar mechanism has to be considered for $CuCl_2$, which can proceed according to the reaction:

$$2CuCl_2 + Cr_2O_3 + 5/2O_2 \rightarrow 2CuCrO_4 + 2Cl_2 \qquad (Eq\ 3)$$
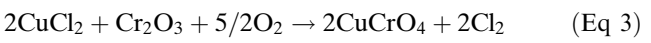
Such a reaction between heavy metal chlorides and chromia prevents the formation of a continuous oxide scale. No protective chromia scale was found on any of the coating surfaces in this study. It would also be interesting to investigate the differences in the flu gas on the behavior and the reactions.

From the results on JB 007 and 2.4856 it is evident that porosity and microstructure of the coatings also play a
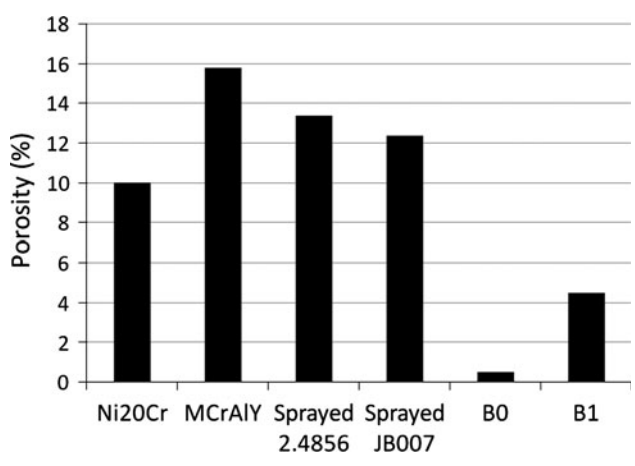

Fig. 7 Porosity of the coatings in the initial state, note the overlay welded coatings are fully dense

critical role, even if the composition is optimized as was shown for waste incineration applications in the case of 2.4856. Although the application of cladding on super heater tubes is more complex than HVOF or flame
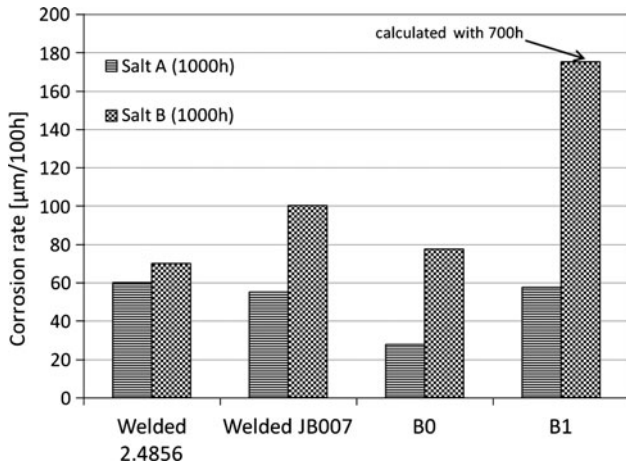
Fig. 8 Corrosion rate per 100 h after exposure in salt A and salt B for the welded and some sprayed coatings

spraying, the results prove that it could be worth the effort and is highly recommended to enhance the corrosion behavior. Still, it would be interesting to investigate if a lower porosity, achieved by an optimized thermal spraying technique, could help to improve the behavior.

Another option is to solidify self-fluxing thermal spray coatings by a heat-treatment, which is a successful approach as demonstrated by the excellent performance of the self-fluxing sprayed coating B0. Such a coating still contains pores, but in contrast to the sprayed coatings it owns a closed porosity. Nevertheless, the composition of the coating also plays a critical role, proven by the two self-fluxing coatings used in this study. Although the exact composition is proprietary, it should be noted that both coatings contain the same elements and were manufactured exactly the same way. Coating B1 disintegrated completely in salt B after 700 h and coating B0 was still resistant. That confirms that the element content and ratio
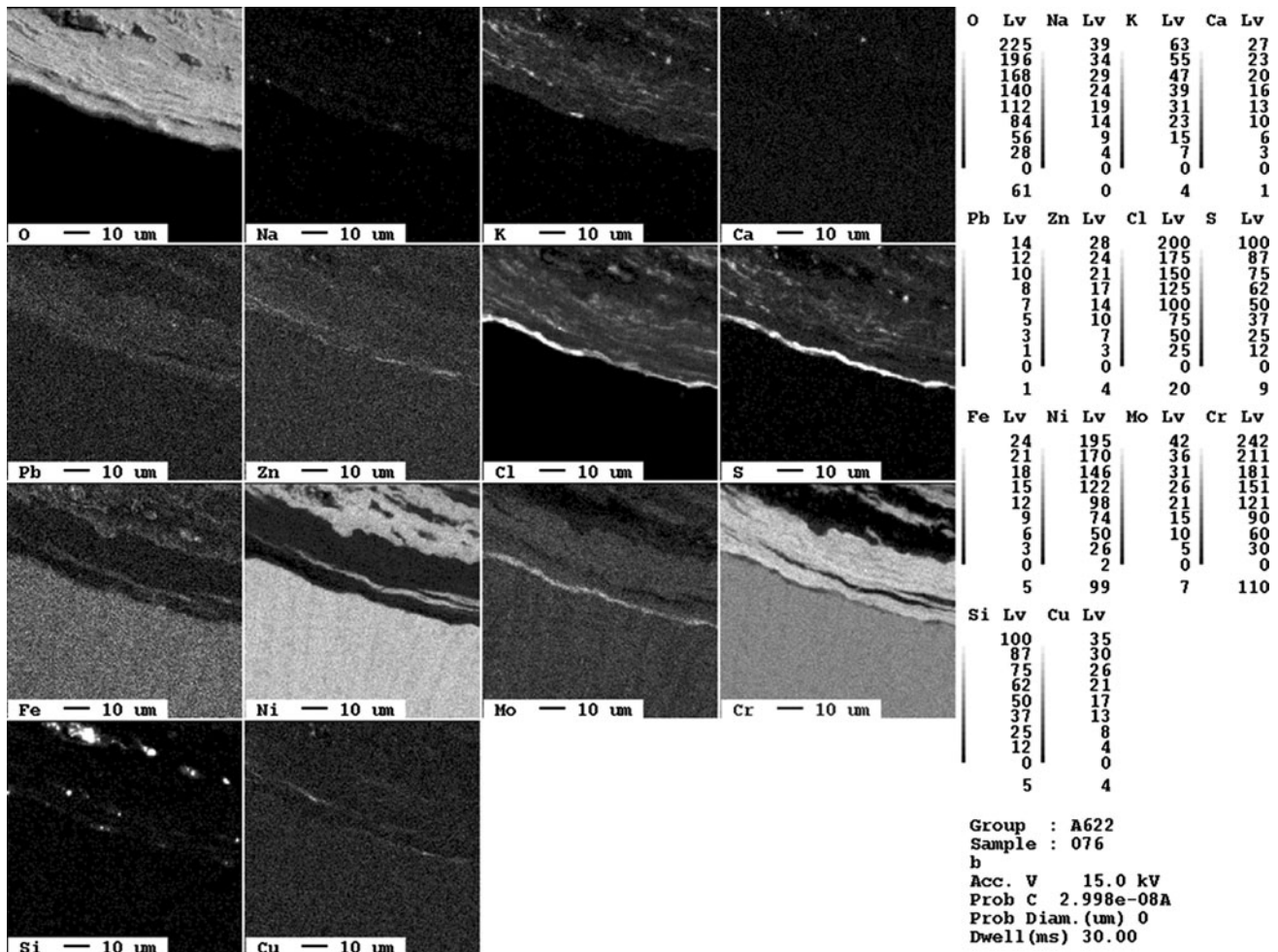

Fig. 9 EMPA of welded 2.4856 after exposure in salt B for 300 h. Beside Cl and S Mo is enriched at the corrosion front under a chromium-rich scale
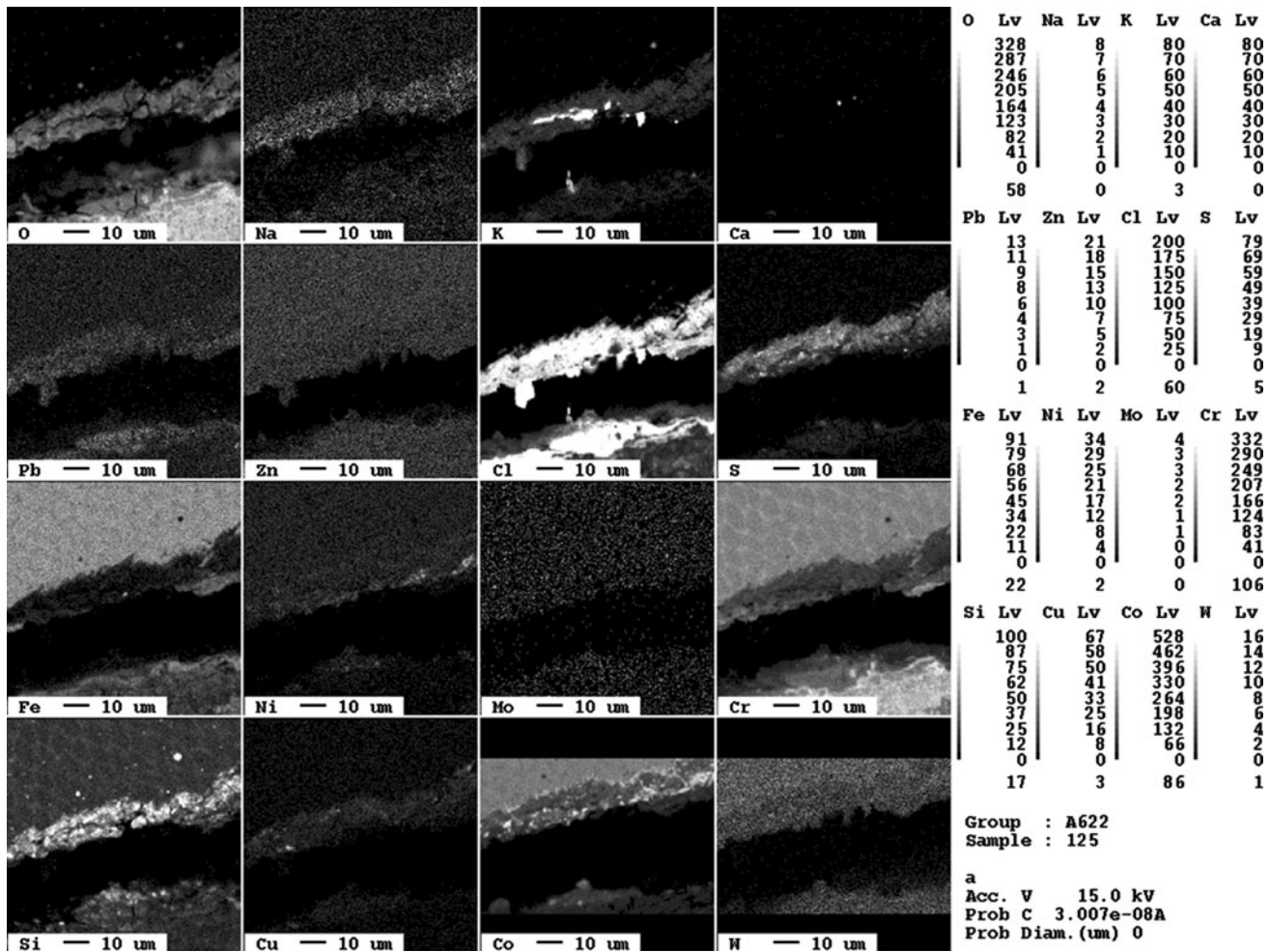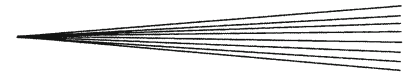
Fig. 10 EMPA of welded JB007 after exposure in salt B for 300 h. Beside Cu, Cl, and S the elements Co and Si from the coating can be found at the corrosion front

of the elements, as well as the resulting microstructure have a high impact on the outcome. In coating B0 a lot of small precipitates can be found, whereas in coating B1, which contains more chromium, less, but larger precipitates are present. This more homogeneous distribution of the protective elements is believed to be a crucial factor for the different behavior.

In general, an interesting difference is the basic concept of the alloying elements in the most resistant coatings. While all contain chromium, either additional molybdenum or silicon seems essential for a good protection. In all coatings a high chromium content is used, which leads to a more or less continuous and protective oxide scale, it was observed for 2.4856 that a continuous molybdenum-rich layer develops at the surface, which furthermore protects the material and lowers the corrosion rate significantly. It was proposed in the literature that this molybdenum-rich layer consists of MoO_2, but enrichments of sulfur and chlorine were also found in this study, therefore this layer should be investigated in more detail. A comparison of the corrosion rate of the 2.4856 coating (70 µm/100 h) with

the bulk material (115 µm/100 h) in salt B, which was reported before (Ref 7), proves that contamination with small amounts iron from the substrate during the welding process does not worsen the corrosion behavior. The coating can still establish the required protective layers, which is in good agreement with the findings of (Ref 17), where it was shown that even 10% alloying with substrate elements does not deteriorate the corrosion behavior of 2.4856. The good performance of 2.4856, which is one of the best coatings even above 500 °C, stands in contrast to Ref 18, where it was stated that 2.4856 should not be exposed to temperatures exceeding 400 °C. While alloying Ni-base material with molybdenum is known to be very efficient in chlorine-rich waste incineration environments (Ref 19), the high corrosion resistance of JB007 and the self-fluxing coatings relies on a rather high silicon content, which leads to an enrichment of silicon close to the surface. This silicon is oxidized to form silicon dioxide and slows down the corrosion rate. For the cobalt-base substrate JB007 a continuous silica layer was found, while for the self-fluxing coating no such continuous layer was
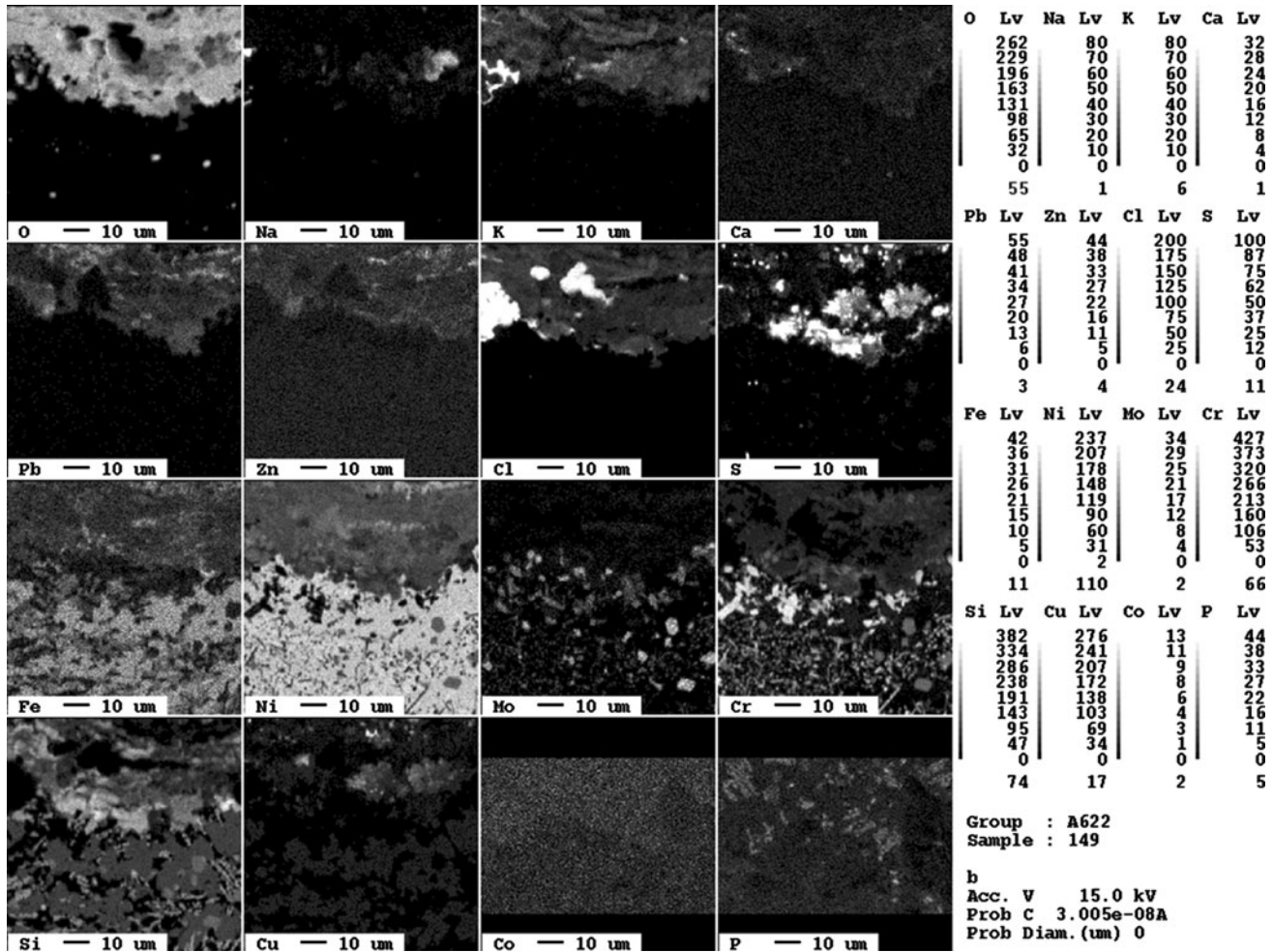
Fig. 11 EMPA of self-fluxing coating B0 after exposure in salt B for 300 h. Cl is at the corrosion front, but no continuous scale of elements of the substrate can be found at the corrosion front

observed, but still they have a protective effect. The concept of alloying either with silicon or with molybdenum in combination with high amounts of chromium seems crucial for a long lifetime, according to the results from this study. The influence of the cobalt content in JB 007 is not clear yet, but it might enhance the formation of a SiO_2 barrier and it is also well known for its high affinity to sulfur. To our knowledge the mutual reaction of cobalt in chlorine- and sulfur-containing atmospheres is not yet investigated, but the good performance of the cobalt-base JB 007 material proves that this class of alloys is of potential interest for such applications and should be investigated in more detail in the future.

Finally, it should be mentioned that the initial thickness of the overlay welded coatings is usually about 2.5-3 times higher than that for sprayed ones. Within this limitation the application of self-fluxing coatings could be an interesting alternative to the established nickel-base claddings, that both show a high resistance, even for heavy metal-induced salt ash attack.

5. Conclusions

Self-fluxing thermal-sprayed coatings and overlay weldings show the lowest corrosion rates under both heavy metal and chloride-rich environments with and without copper.

The porosity of sprayed coatings plays a critical role for the corrosion resistance of coatings in WTPs. It was shown to be especially important for higher chlorine and heavy metal contents in the deposits, which lead to a lowering of the melting point and therefore lower viscosity at service temperature that can easily penetrate such scales.

A high content of the alloying elements silicon and molybdenum is required for a low rate of corrosive attack, but it must be ensured that the technology by which such systems are applied leads to fully dense scales, or at least a closed porosity.

In contrast to observations reported in the literature, 2.4856 showed a very high resistance, although exposed to 540 °C, which was reported previously to be too high for

this alloy (Ref 18). Although the price of overlay welded alloys as well as that of self-fluxing spray coatings is higher than that of flame-sprayed or HVOF coatings, the higher manufacturing expenses are partly compensated by avoiding the cost of refractory maintenance.

The influence of variations in the amount of heavy metals in the ash and the sulfur/chlorine ratio in the gas should be investigated in further experiments, as WTPs run on an extremely inhomogeneous feed stock and it is not yet possible to predict the behavior when these conditions change. Nevertheless, the findings prove that especially in environments were the feedstock contains high amounts of chlorine and copper, self-fluxing coatings or overlay weldings can significantly extend the lifetime of the system.

References

1. P. Rademakers, W. Hesseling, and J. van de Wetering, "Review on Corrosion in Waste Incinerators, and Possible Effect of Bromine," TNO Industrial Technology, Report, 2002
2. C.C.Y. Chan and D.W. Kirk, Behaviour of Metals Under the Conditions of Roasting MSW Incinerator Fly Ash with Chlorinating Agents, *J. Hazard. Mater.*, 1999, **64**(1), p 75-89
3. S. Biollaz, C. Ludwig, M. Beckmann, M. Davisovic, and T. Jentsch, Volatility of Zn and CU in waste incineration: radio-tracer experiments on a pilot incinerator, *Proceedings Incineration and Thermal Treatment Technologies*, Portland, USA, 2000
4. C. Ferreira, A. Ribeiro, and L. Ottosen, Possible Applications for Municipal Solid Waste Fly Ash, *J. Hazard. Mater.*, 2003, **96**(2-3), p 201-216
5. L.S. Morf, P.H. Brunner, and S. Spaun, Effect of Operating Conditions and Input Variations on the Partitioning of Metals in a Municipal Solid Waste Incinerator, *Waste Manage. Res.*, 2000, **18**(1), p 4-15
6. S.H. Lee, N. Themelis, and M. Castaldi, High-Temperature Corrosion in Waste-to-Energy Boilers, *J. Therm. Spray Technol.*, 2007, **16**(1), p 104-110
7. M.C. Galetz, J.T. Bauer, M. Schütze, M. Noguchi, C. Takatoh, and H. Cho, The Influence of Copper in Ash Deposits on the Corrosion of Boiler Tube Alloys for Waste-to-Energy Plants, *Mater. Corros.*, 2012, doi:10.1002/maco.201206787
8. C.M. Fontana, E. Gorin, G.A. Kidder, and C.S. Meredith, Chlorination of Methane with Copper Chloride Melts, *Ind. Eng. Chem.*, 1951, **44**(2), p 363-368
9. M. Spiegel, A. Zahs, and H.J. Grabke, Fundamental Aspects of Chlorine Induced Corrosion in Power Plants, *Mater. High Temp.*, 2003, **20**, p 153
10. J. Bertholt, "Metal Body with Metallic Protective Coating," EP2113578A2, 2008
11. A.J. Chandler, T.T. Eighmy, J. Hartlén, O. Hjelmar, D.S. Kosson, S.E. Sawell, H.A. Van der Sloot, and J. Vehlow, *Municipal Solid Waste Incinerator Residues (Studies in Environmental Science)*, Vol 67, Elsevier, Amsterdam, 1997
12. S. Deshpande, A. Kulkarni, S. Sampath, and H. Herman, Application of Image Analysis for Characterization of Porosity in Thermal Spray Coatings and Correlation with Small Angle Neutron Scattering, *Surf. Coat. Technol.*, 2004, **187**, p 6-16
13. D.B. Fowler, W. Riggs, and J.C. Russ, Inspecting Thermal Sprayed Coatings, *Adv. Mater. Process.*, 1990, **11**, p 41-52
14. I.A. Suleiman, J.C. Mackie, E.M. Kennedy, M.W. Radny, and B.Z. Dlugogorski, Quantum Chemical Study of Copper (II) Chloride and the Deacon Reaction, *Chem. Phys. Lett.*, 2011, **501**, p 215-220
15. M. Spiegel, Salt Melt Induced Corrosion of Metallic Materials in Waste Incineration Plants, *Mater. Corros.*, 1999, **50**, p 373-393
16. D. Bankiewicz, S. Enestam, P. Yrjas, and M. Hupa, Experimental Studies of Zn and Pb Induced High Temperature Corrosion of Two Commercial Boiler Steels, *Fuel Process. Technol.*, 2013, **105**, p 89–97
17. J. Adamiec, High Temperature Corrosion of Power Boiler Components Cladded with Nickel Alloys, *Mater. Charact.*, 2009, **60**(10), p 1093-1099
18. W. Spiegel, T. Herzog, W. Müller, and W. Schmidl, Praxisnahe Unterstützung der Betreiber bei der Optimierung und nachhaltigen Nutzung der bayerischen MV-Anlagen. Bayerisches Landesamt für Umweltschutz, Report, 2002
19. Y. Kawahara, High Temperature Corrosion Mechanisms and Effect of Alloying Elements for Materials Used in Waste Incineration Environment, *Corros. Sci.*, 2002, **44**, p 223-245